Earth Systems and Environment (2018) 2:367–375
https://doi.org/10.1007/s41748-018-0053-y

ORIGINAL ARTICLE

Monitoring of Water-Level Fluctuation of Lake Nasser Using Altimetry Satellite Data

Mohammed A. El-Shirbeny[1] · Khaled A. Abutaleb[1,2]

Received: 7 November 2017 / Accepted: 22 May 2018 / Published online: 28 May 2018

Abstract
Apart from the Renaissance Dam and other constructed dams on the River Nile tributaries, Egypt is classified globally as a state of scarce water. Egypt's water resources are very limited and do not contribute a significant amount to its water share except the River Nile (55.5 billion m^3/year). While the number of population increases every year, putting more stress on these limited resources. This study aims to use remote-sensing data to assess the change in surface area and water-level variation in Lake Nasser using remote-sensing data from Landsat-8 and altimetry data. In addition, it investigates the use of thermal data from Landsat-8 to calculate water loss based on evaporation from Lake Nasser. The eight Landsat-8 satellite images were used to study the change in surface area of Lake Nasser representing winter (January) and summer (June/July) seasons in two consecutive years (2015 and 2016). Time series analyses for 10-day temporal resolution water-level data from Jason-2/OSTM and Jason-3 altimetry was carried out to investigate water-level trends over the long term (1993 and 2016) and short term (2015–2016) in correspondence with the change of the surface area. Results indicated a shrink in the lake surface area in 2016 of approximately 14% compared to the 2015 area. In addition, the evaporation rate in the lake is very high causing a loss of approximately 20% of the total water share from the river Nile.

Keywords Water scarcity · Altimetry data · Lake Nasser · Flooding and drought

1 Introduction

The Nile River is the longest river worldwide. It travels about 7000 km long. The water travels from the upstream countries (South Sudan, Burundi, Ethiopia, Uganda, Eretria, Kenya, Tanzania, Rwanda, and the Democratic Republic of Congo) towards the downstream countries (Egypt, North Sudan). The River Nile has two major tributaries, the White Nile and the Blue Nile. The discharge of the White Nile is approximately constant over the whole year, while the Blue Nile gives more than 80% of its share between July and August during the rainy season in the highlands of Ethiopia (Abd-El Monsef et al. 2015).

When the Soviet Union offered to build the Aswan high dam in 1958, the construction was started in 1964, and it was completed in 1970. The dam height is 111 m. The fill-up of the reservoir took 6 years. The name of Lake Nasser is given to this reservoir. Lake Nasser/Nubia extends over 500 km long, and 6000 km^2 surface area and water level reach 182-m above sea level in case of full storage scenario (Muala et al. 2014). That makes it a gigantic man-made reservoir (ElKobtan et al. 2016). It can store up to 130 billion m^3 of water. Apart from this amount, 32 km^3 is dead storage, leaving enough live storage to satisfy Egypt's agricultural and domestic needs from water (Kamel and Elsirafe 1993; Abd-El Monsef et al. 2015).

Egypt as it is classified as a dry arid area with infrequent rainfall events. The minimum temperature is 5 °C in January and the maximum temperature reaches as high as 45 °C in July (Kottek et al. 2006). Thus, the loss of surface water by high evaporation rate is a serious problem during this time of the season. Egypt agriculture lands are concentrated in the Nile delta and the Nile valley. Agriculture plays an essential role in Egypt's economy. It employs more than 25.6% of the labor force and contributes by 25% of the national GDP (CAPMAS 2018a, b). The agricultural system depends entirely on irrigation. About 86% of the water delivered from

✉ Khaled A. Abutaleb
abutalebk@arc.agric.za

1 National Authority for Remote Sensing and Space Sciences, Cairo, Egypt

2 Institute for Soil, Climate and Water, ARC, Pretoria, South Africa

the Nile is used for agricultural purposes (FAO-Aquastat 2015).

Satellite data are found very useful in natural resource monitoring and management, since it provides a wide spatial extent and temporal coverage. Unlike traditional field survey, mapping using remote sensing is not constrained by rough inaccessible terrains or geopolitical boundaries and it provides access to extensive historical data archives for retrospective studies. Remote sensing is up to date, cost effective, non-destructive and timely (El-Shirbeny et al. 2014a, b; Misra et al. 2013; Misra and Balaji 2015; Muala et al. 2014; Sundarakumar et al. 2012; Zhang and Zhu 2011). Satellite altimetry is a remote-sensing technique which has been used to derive water-level data for approximately two decades (Cretaux and Birkett 2006). Integrating satellite altimetry and satellite remote sensing has become a potential technique for hydrological monitoring and water resource management (Alsdorf et al. 2007; Arsano and Tamrat 2005; Calmant et al. 2008; Cretaux and Birkett 2006; Duan and Bastiaanssen 2013; Gerlak et al. 2011; Medina et al. 2010; Muala et al. 2014; Zhang et al. 2006). Muala et al. (2014) investigated three different data sets (altimetry, optical imagery, and in situ data) to compare between the Roseries Reservoir and Lake Nasser water volume variations. They found a high correlation between the altimetry and in situ data sets but a weak correlation between the in situ data and the volume estimation from satellite imagery.

The aim of this study was to investigate the surface area and the water-level variations in Lake Nasser during the flooding and drought seasons using remote sensing and Jason-2/OSTM and Jason-3 altimetry data, respectively, for the period of 1993–2016.

2 Materials and Methods

2.1 Geographic Location

Lake Nasser is a huge artificial reservoir share the border between Egypt and Sudan. The water accumulation behind the Aswan high dam created the lake (Fig. 1). It is located between 20.45 and 23.97N and 30.12 and 33.25E. It has an average range of temperature of 5 °C in winter and 45 °C during summer. The area is classified as hyper-arid with infrequent rainfall events (Kottek et al. 2006).

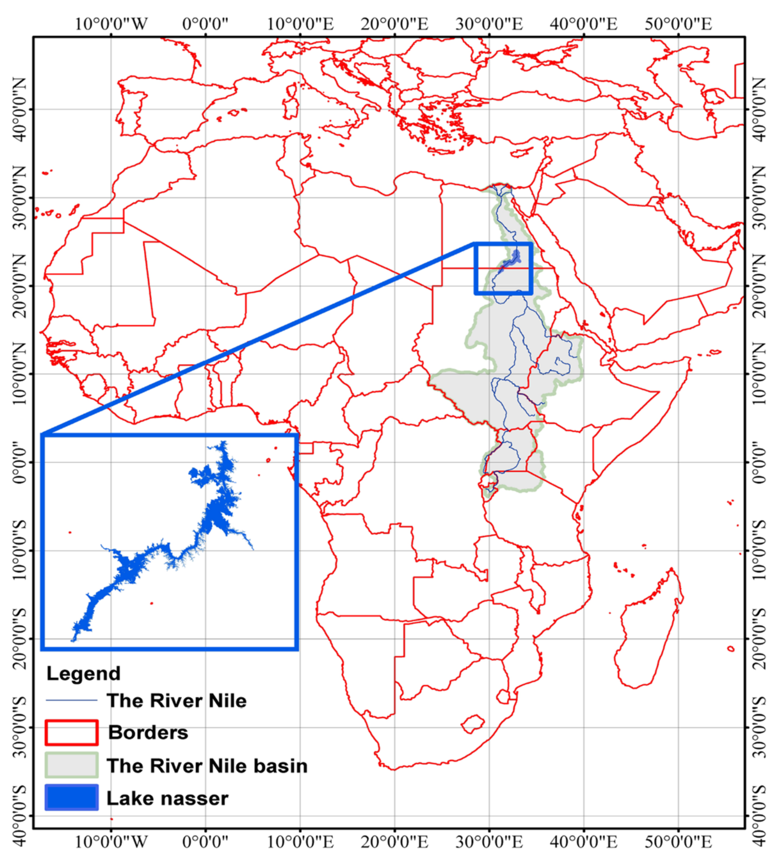

Fig. 1 Geographic location of Lake Nasser

2.2 Data Collection

2.2.1 Altimetry Data

Understanding water storage changes within the Nile's main basin and sub-basins is an essential step in managing its water resources (Awange et al. 2014). A 10-day temporal resolution from January 2015 to July 2016 used to monitor the relative variations in surface water level in Lake Nasser. The relative lake height variations computed from Jason-2/OSTM and Jason-3 altimetry data.

The water level in Roseires reservoir (Sudan) and Lake Nasser (Egypt) using satellite altimetry and in situ data was studied by (Muala et al. 2014). They observed that the altimetry data of − 6.21 and + 5.96 m and is equal to 169.24 and 181.41 m based on in situ data. According to Muala et al. (2014) results, the altimetry data of zero is equal to 175.45 m.

To analyze the water level for different time spans, different summary statistics were calculated using the R software packages. The monthly, seasonal, and annual average water levels were estimated from the original 10-day data. The monthly data were calculated by averaging the 10-day readings fall in the month for each year, and then, the seasonal data were calculated by averaging the monthly data for each season and the annual data were also calculated from the monthly data for each year.

2.2.2 Digital Elevation Model (DEM)

The Advanced Space-Borne Thermal Emission and Reflection Radiometer (ASTER) Global DEM Version 2 with 30-m resolution (https://asterweb.jpl.nasa.gov/gdem.asp) was used to describe the topographical features of the reservoir using the arc map 10.1 software. The elevation data varied from 100 to 1158 m (Fig. 2). The 175.4-m contour line was extracted from DEM through the ENVI 5.1 software (Fig. 3). The 175.4 m was chosen as the baseline for the water levels provides by Jason-2/OSTM and Jason-3 altimetry data, i.e., the positive value of 2 means water level of 177.4 m front of the high dam and so on.

2.2.3 Surface Water Area Changes

Four different dates Landsat-8 satellite images were acquired for January and June 2015 and 2016 (Table 1) to map and identify the changes of the surface area of Lake Nasser during flooding and dry seasons in the two consecutive years. Landsat-8 Operational Land Imager (OLI) has the spatial resolution of 30 m and a high spectral resolution of 11 channels giving it an advantage for many applications and characterizations (Table 2). The images are geometrically corrected to the Universal Transverse

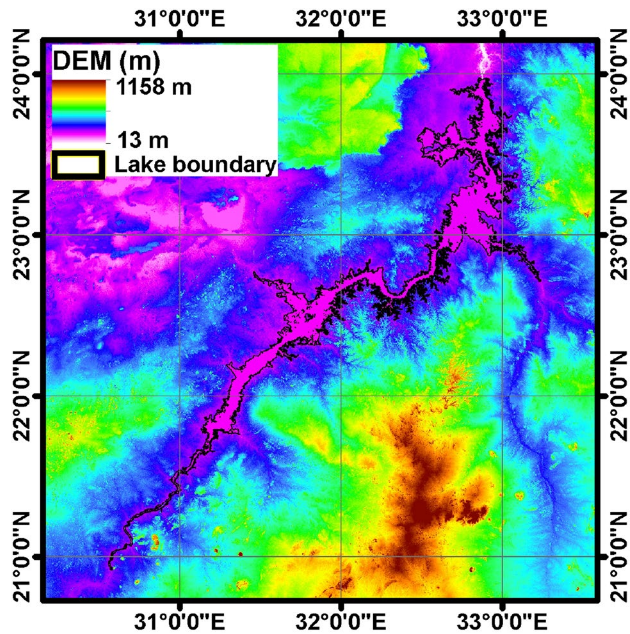

Fig. 2 The 175.4-m contour line and boundary extension of the lake at the highest recorded water level (181.41 m)

Table 1 Satellite images path/row and dates

Path	Row	Date	Path	Row	Date
174	044	15 January 2015	174	044	02 January 2016
175	044	06 January 2015	175	044	09 January 2016
175	045	06 January 2015	175	045	09 January 2016
174	044	10 July 2015	174	044	10 June 2016
175	044	01 July 2015	175	044	17 June 2016
175	045	01 July 2015	175	045	17 June 2016

Mercator (UTM) grid system, Zone 36 North, and the WGS84 datum. Image classification was carried out using the ENVI and ArcGIS software. Two classification methods were used in the delineation of the lake body. The first method is based on the Normalized Difference Water Index (NDWI) given by McFeeters (1996) Eq. (1). Hence, the land cover of the study area is not heterogeneous. It is either water or mountainous areas with submerged vegetation on the lake boundaries. Calculating the NDWI will give one band image with high values at areas of water and less otherwise. A threshold was used to delineate the water body in combination with the DEM:

$$\mathrm{NDWI} = \frac{\mathrm{Green} - \mathrm{NIR}}{\mathrm{Green} + \mathrm{NIR}}. \quad (1)$$

The other method applies the Normalized Difference Vegetation Index (NDVI) (Kriegler et al. 1969; Rouse et al. 1973) which is the opposite of the NDWI (Eq. 2).

Table 2 Landsat-8 OLI spectral, spatial characteristics and application (Barsi et al. 2014)

Band	Wavelength (μm)	Application	Resolution (m)
Band 1—coastal–aerosol	0.435–0.451	Coastal and aerosol studies	30
Band 2—blue	0.452–0.512	Bathymetric mapping, discriminate between soil and vegetation, and deciduous from coniferous vegetation	30
Band 3—green	0.533–0.590	Assessment of plant vigor	30
Band 4—red	0.636–0.673	Discriminates vegetation slopes	30
Band 5—Near Infrared (NIR)	0.851–0.879	Biomass content and shorelines	30
Band 6—Short-Wave Infrared (SWIR) 1	1.566–1.651	Discriminates moisture content of soil and vegetation; penetrates thin clouds	30
Band 7—Short-Wave Infrared (SWIR) 2	2.107–2.294	Improved moisture content of soil and vegetation and thin cloud penetration	30
Band 8—panchromatic	0.503–0.676	Sharper image definition	15
Band 9—cirrus	1.363–1.384	Improved detection of cirrus cloud contamination	30
Band 10—TIRS 1	10.60–11.19	Thermal mapping and estimated soil moisture	100[a] (30)
Band 11—TIRS 2	11.50–12.51	Improved thermal mapping and estimated soil moisture	100[a] (30)

[a]TIRS bands are acquired at 100-m resolution, but are resampled to 30 m

NDVI for water is very low as water absorbs big portions of the NIR band resulting in very low negative values of NDVI:

$$\mathrm{NDVI} = \frac{\mathrm{NIR} - \mathrm{Red}}{\mathrm{NIR} + \mathrm{Red}}. \tag{2}$$

2.2.4 Evaporation Estimation

Evaporation rates were calculated as a point estimates using the meteorological data provided by the weather stations at Aswan and Abu-Simbel. Equation (3) gives the mathematical representation of how evaporation rate was calculated. The Penman formula for the evaporation rate from a lake is simplified to the following (Linacre 1977):

$$E_{\mathrm{o}} = \frac{700\frac{T_{\mathrm{m}}}{100-A} + 15(T - T_{\mathrm{d}})}{(80 - T)}(\mathrm{mm\ day}^{-1}) \tag{3}$$

where T is the mean temperature, h is the altitude, A is the latitude, T_{d} is the mean dew point, and $T_{\mathrm{m}} = T + (0.006 \times h)$. Although this equation is applicable to a wide range of climatic zones and conditions, the values given by this formula differs slightly from the actual measurements (0.3 0.5, 0.9, and 1.7 mm/day from the annual, monthly, weekly, and daily mean, respectively):

$$(T - T_{\mathrm{d}}) = 0.0023h + 0.37T + 0.53R + 0.35R_{\mathrm{ann}} - 10.9\,^{\circ}\mathrm{C} \tag{4}$$

where R is the average daily temperature and R_{ann} is the difference between the average maximum and the average minimum temperatures.

3 Results and Discussion

3.1 Surface Water Area Changes

The surface area of Lake Nasser (Fig. 3) is obtained using eight Landsat-8 scenes. The two dates represent the two different cases of the lake, i.e., the flooding season which occurs during winter represented in January in this study, while the other date represents the dry season taking place during summer represented in June in the current study. Data illustrated in Table 3 show the area of each selected date in square kilometers.

Data reveal a decrease in the surface area when comparing two consecutive dry or flooding seasons. The decrease in area means the reduction in water level in front of the high dam. The lake lost approximately 1230 km^2 from January 2015 to June 2016. The fact about the fluctuation of water levels could be due to the flooding and the dry seasons is true but comparing both dry and flooding season in the study period reflects that the Lake lost approximately 666 km^2 from January 2015 to January 2016, which indicates a reduction on the inflow of the upstream countries. This may be attributed to the construction of the new dams in the upstream countries such as the Renaissance Dam which commenced in 2011. The other fact is comparing the surface area of the dry season of 2015 with the flooding season of 2016 that it reveals a loss of roundly 411 km^2 in the surface area of Lake Nasser. The fact the evaporation is proportional to the surface area, so the difference between the change between the two seasons, i.e., changes between flooding season of 2015 and the same season of 2016 (666 km^2) and change between dry season of 2015

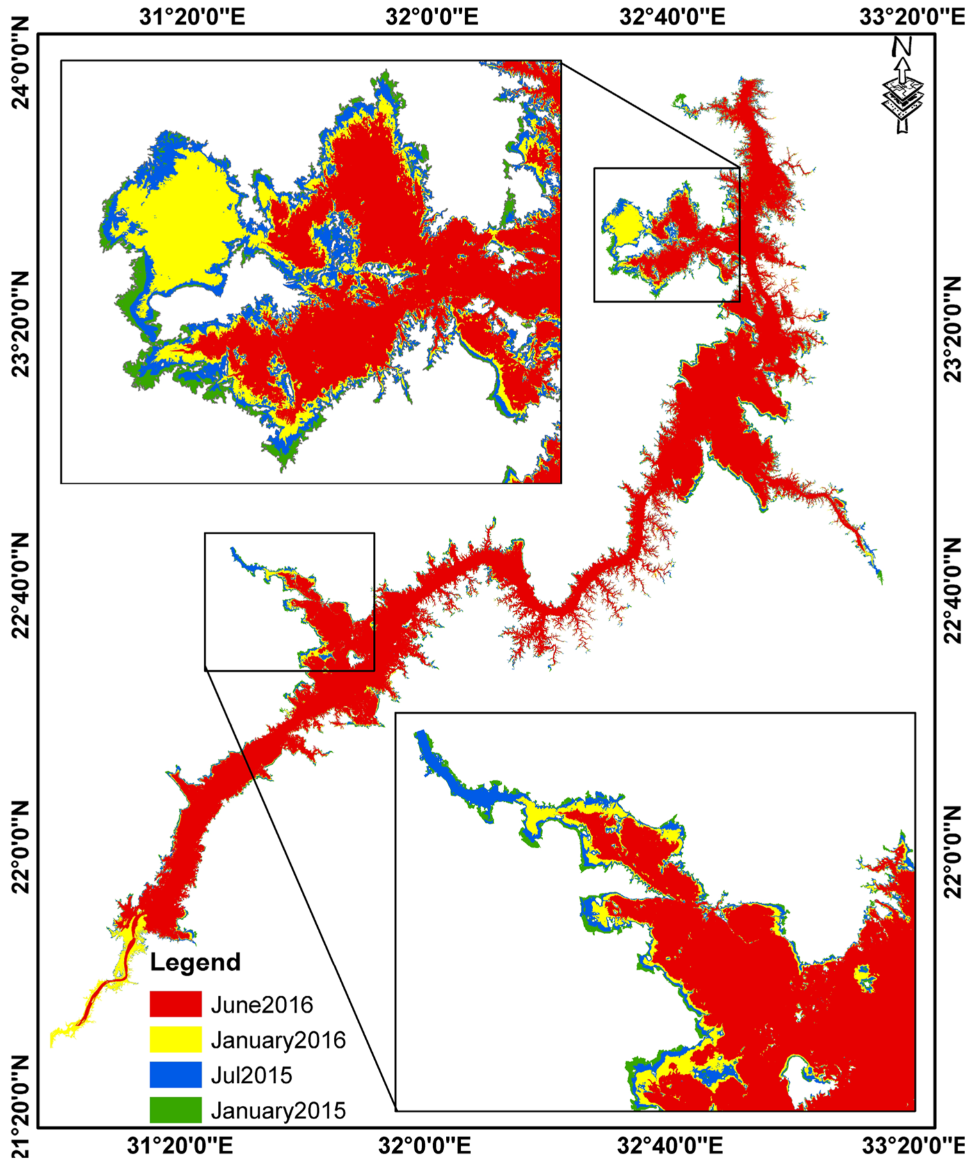

Fig. 3 Changes in Lake Nasser surface area

Table 3 Lake Nasser surface area in 2015 and 2016

Date	Area (Km^2)
January 2015	5637.53
July 2015	5382.17
January 2016	4971.12
June 2016	4407.66

and 2016 (411 km^2) could be attributed to the reduction of evaporation.

3.2 Water Level of Nasser Lake

Figures 4 and 5 and Table 4 summarize the summary statistics about the 10-day, monthly, seasonal, and annual averaged data as a time series for 24 years (1993–2016). The highest water level was 6.4 m recorded on 27-December-1999 and the lowest (−5.64 m) was recorded on the 1st of July 1993. The lowest water level was recorded in 1993, while the highest level was recorded in 2000. Figure 4h reveals that the lowest season is the spring season, while autumn is the highest season with means of −0.952 and 2.131 m, respectively. From the yearly data (Fig. 4j), year 1993 was the lowest water level with water level (−3.64 m), while year 2000 was the highest level (3.652 m). Monthly speaking (Fig. 4e), November and July were the maximum and the minimum in terms water level (2.229 and −1.906 m), respectively.

Figure 5 shows the curve reflects the fact that the sinusoidal behavior of the lake through the two seasons (flooding and dry seasons). For clarity, the curve in Fig. 5 will be divided into two parts a and b, where part (a) represents

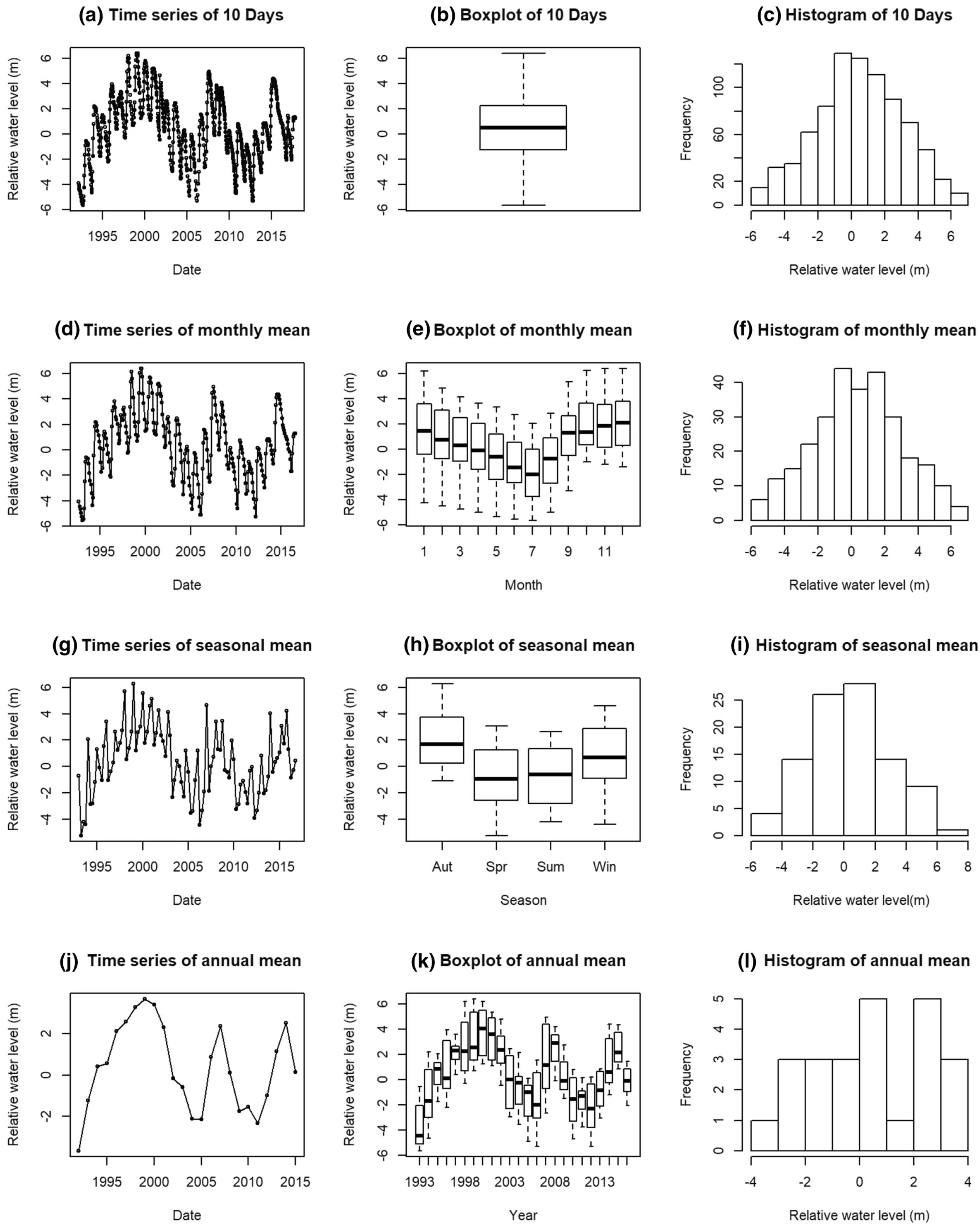

Fig. 4 10-day monthly, seasonal, and annual data exploration for the relative water level of Lake Nasser

the years from 1992 to 2005 and part (b) represents years from 2006 to 2016. The first interval has a characteristic of very narrow wavelength which means that the time between to events from the same type (i.e., flood or dry) is short, while part (b) is characterized by long wavelengths, which mean that the reservoir refill takes longer time compared by the 1992–2005 interval. These fluctuations in the flow have a great effect on the agriculture and food security in Egypt (McSweeney et al. 2010; El-Shirbeny et al. 2014b).

In more details, Fig. 6 and Table 4 give the water levels of the current study period (2015–2016). It is clear that water level during the 2 years is decreasing. In 2016, water levels are below the baseline (175.4 m). This may be due to the Ethiopian millennium dam which under construction and partial fill of its reservoir. Although the negotiations between the Egyptians and the Ethiopians regarding the fill time, it seems the noticeable reduction of Egypt water share no way to be avoided. Figure 6 also gives a representation of the surface area decrease in correspondence with the water levels.

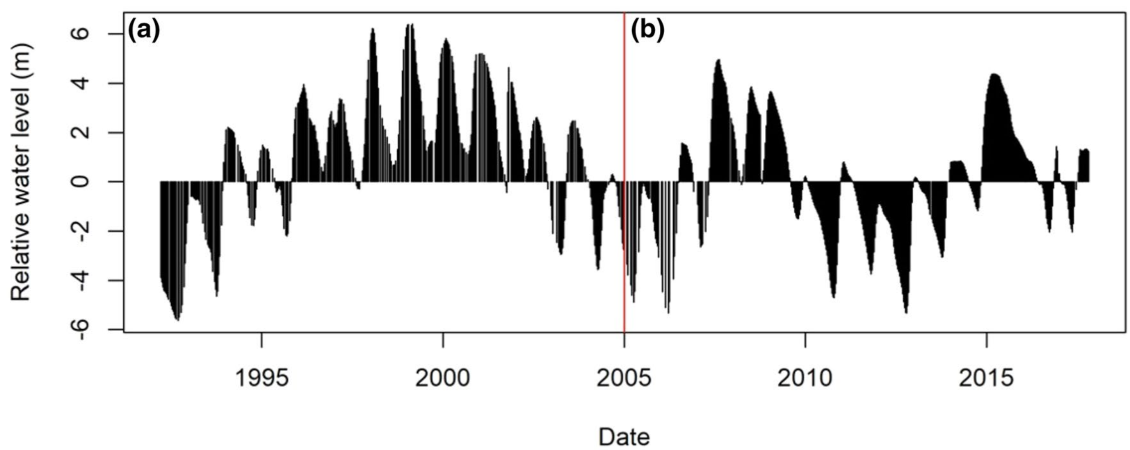

Fig. 5 Water levels of Lake Nasser **a** from 1992 to 2005, **b** from 2006 to 2016

Table 4 10-day monthly, seasonal, and annual mean data summary statistics

	Median	Mean	SD	First Qu	Third Qu.	Min.	Date	Max.	Date
10 days	0.500	0.484	2.618	− 1.230	2.273	− 5.640	01-July-1993	6.400	27-December-1999
Month	0.394	0.375	2.676	− 1.377	2.139	− 5.535	June 1993	6.380	November 1999
Season	0.427	0.375	2.603	− 1.209	2.005	− 5.249	Spring 1993	6.272	Autumn 1999
Year	0.275	0.375	2.201	− 1.299	2.302	− 3.644	1993	3.652	2000

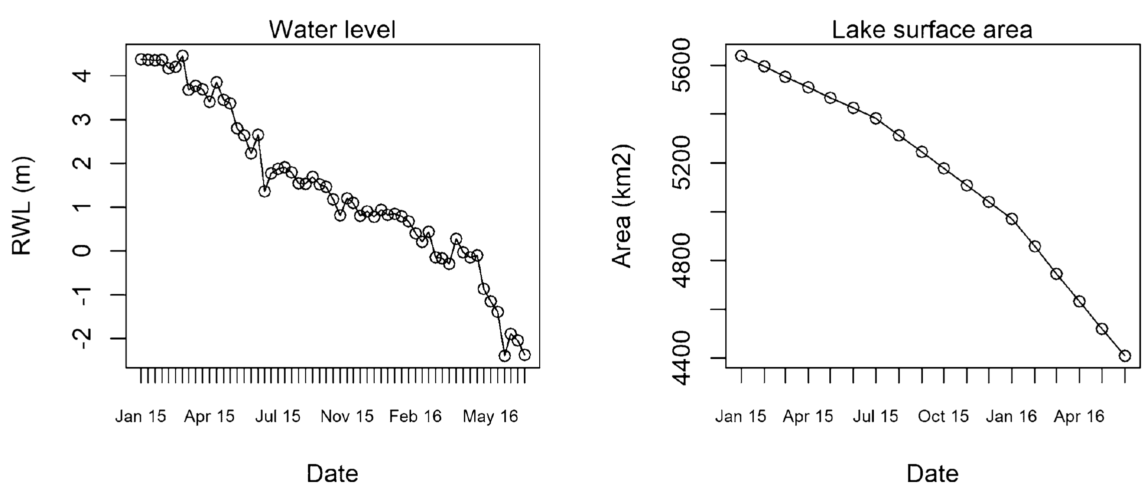

Fig. 6 Water level and the interpolation of the surface area of the study time interval

The monthly area was achieved by the linear interpolation of the area decrease between two studied dates. A fact that the water level in 2016 is still higher than the minimum recorded along the period of 1993 up to date which is (−5.640 m) at 1st of July 1993.

Table 5 summarizes the Mann–Kendell (Hirsch et al. 1982) statistics for the water-level data from January 2015 to December 2016. The statistical analysis revealed the negative correlation between water levels and time which indicates a negative trend of magnitude of −0.24-m monthly in the water level of Lake Nasser. This result is in agreement with the surface water area estimation from satellite data (Leon et al. 2006; Muala et al. 2014; Swenson and Wahr 2009).

3.3 Evaporation Rates

The evaporation rate in Lake Nasser is very high (Fig. 7). This may be attributed to its large extent as well as the surrounding land cover which is sand and rock desert. Abutaleb et al. (2015) state that the bare soil and sandy rocky areas possess higher land surface temperature than the vegetation land covers. This in turn increases the microclimate temperature and leads to higher evaporation rates. Bastawesy et al. (2008) studied the volume of water losses of Tushka lakes which not far from Lake Nasser, and they found a significant rate losses because of evaporation and infiltration.

The evaporation rates in Lake Nasser ranged between 120 and 410 mm/month. It is a minimum in the winter months, while it is very high in the summer months. It reaches the maximum on August. To calculate the total water loss in cubic meters, the evaporation rate is multiplied by the corresponding lake area estimated from the satellite images. This high evaporation rates cause the lake to lose about (0.6–1.9) billion m^3 a month. Taking the average of these two numbers and multiplying it by 12 months will result in 15 billion m^3 loss per year which represents 20% of Egypt share from the river Nile.

4 Conclusion

The use of remote sensing has been proven to be an accurate and effective tool in environmental monitoring and management. The use of four different Landsat-8 images in two consequent seasons for 2 years gives opportunity for monitoring the surface area change in Lake Nasser which is a huge water body. In addition, the altimetry data derived from remote-sensing data also gave insight of the relative water level behind the high dam at Aswan along 24 years. In developing countries such as Egypt, it is very difficult to know whether these data are available or not and might be impossible to get such long continues data set. The lake surface area has shrunk from 5637.53 km^2 in January 2015 to 4971.12 km^2 in January 2016. The relative water level in Lake Nasser is the minimum during summer season with seasonal mean of −0.952 m, while it is the maximum during autumn with average of 2.131 m. The highest water level recorded during the past 24 years was 6.64 m in December 1999, while the lowest one was −5.64 m in July 1993. The year 1993 was the

Table 5 Mann–Kendall trend test for the water levels (2015–2016)

Standard deviation	Max	Min	Kendall's tau	S'	Var(S')	p value (two-tailed)	Sen's slope
1.70	4.4	−1.70	−0.64	−177.0	1624.3	1.26e−05	−0.24

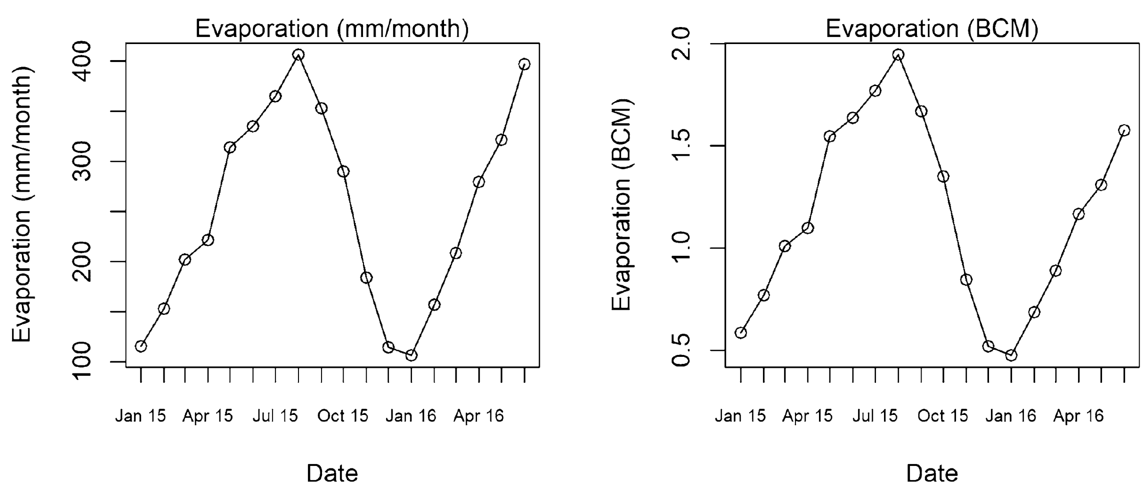

Fig. 7 Evaporation rates and volumes of Lake Nasser during the study time interval

lowest mean water level and the year 2000 was the highest (-3.64 and 3.652 m, respectively). The evaporation rate in Lake Nasser is very high and it is ranging between 120 and 410 mm/month. This is causing the loss of approximately 15 billion m^3 per year.

References

Abd-El Monsef H, Scot ES, Kamal D (2015) Impacts of the Aswan high dam after 50 years. Water Resour Manag 29:1873–1885

Abutaleb K, Ngie A, Darwish A, Ahmed M, Arafat S, Ahmed F (2015) Assessment of urban heat island using remotely sensed imagery over Greater Cairo, Egypt. Adv Remote Sens 4(4):35–47

Alsdorf DE, Rodriguez E, Lettenmaier DP (2007) Measuring surface water from space. Rev Geophys 45:1–24

Arsano Y, Tamrat I (2005) Ethiopia and the Eastern Nile Basin. Aquat Sci 67:15–27

Awange JL, Forootan E, Kuhnm M, Kusche J, Heck B (2014) Water storage changes and climate variability within the Nile Basin between 2002 and 2011. Adv Water Res 73:1–15

Barsi JA, Lee K, Kvaran G, Markham BL, Pedelty JA (2014) The spectral response of the Landsat-8 operational land imager. Remote Sens 6:10232–10251

Bastawesy MA, Khalaf FI, Arafat SM (2008) The use of remote sensing and GIS for the estimation of water loss from Tushka lakes, southwestern desert, Egypt. J Afr Earth Sci 52(3):73–80

Calmant S, Seyler F, Cretaux JF (2008) Monitoring continental surface waters by satellite altimetry. Surv Geophys 29:247–269

CAPMAS (2018a) Egypt in figures-labor: central agency for public mobilization and statistics. CAPMAS, Cairo

CAPMAS (2018b) Egypt in figures-economy: central agency for public mobilization and statistics. CAPMAS, Cairo

Cretaux JF, Birkett C (2006) Lake studies from satellite radar altimetry. Comp Rend Geosci 338:1098–1112

Duan Z, Bastiaanssen WG (2013) Estimating water volume variations in lakes and reservoirs from four operational satellite altimetry databases and satellite imagery data. Remote Sens Environ 134:403–416

El-Gammal EA, Salem SM, El-Gammal AA (2010) Change detection studies on the world's biggest artificial lake (Lake Nasser, Egypt). Egyptian J Remote Sens Space Sci 13:89–99

ElKobtan H, Salem M, Attia K, Ahmed S, Abou-Elmagd I (2016) Sedimentological study of Lake Nasser; Egypt, using integrated improved techniques of core sampling, X-ray diffraction and GIS platform. Cogent Geosci 2:1168069

El-Shirbeny MA, Aboelghar MA, Arafat SM, El-Gindy AGM (2014a) Assessment of the mutual impact between climate and vegetation cover using NOAA-AVHRR and Landsat data in Egypt. Arab J Geosci 7(4):1287–1296

El-Shirbeny MA, Abutaleb KA, Saleh NH, Ali AM (2014b) Water monitoring in Lake Nasser using satellite data. Second New Nile scientific conference, Addis Ababa, Ethiopia. 12/2014. https://doi.org/10.13140/rg.2.1.2048.6241

FAO-Aquastat (2015) Food and agriculture organization of the United Nations. Retrieved from FAO-Aquastat. Country Profile: Egypt. http://www.fao.org/nr/water/aquastat/countries_regions/EGY/index.stm

Gerlak A, Lautze J, Giordano M (2011) Water resources data and information exchange in transboundary water treaties. Int Environ Agreem Polit Law Econ 11:179–199

Hirsch R, Slack J, Smith R (1982) Techniques of trend analysis for monthly water quality data. Water Resour Res 18:107–121

Kamel AF, Elsirafe AM (1993) Delineation and analysis of the surface and subsurface structural lineament patterns in the North Lake Nasser area and its surroundings, Aswan, Upper Egypt. Int J Remote Sens 15(7):1471–1493

Kottek M, Grieser J, Beck C, Rudolf B, Rubel F (2006) World map of the Köppen–Geiger climate classification updated. Meteorol Z 15(3):259–263

Kriegler FJ, Malila WA, Nalepka RF, Richardson W (1969) Preprocessing transformations and their effects on multispectral recognition. In: Proceedings of the sixth international symposium on remote sensing of environment, University of Michigan, Ann Arbor, MI, pp 97–131

Leon JG, Calmant S, Seyler F, Bonne M, Cauhope M, Frappart F, Filizola N, Fraizy P (2006) Rating curves and estimation of average water depth at the upper Negro River based on satellite altimeter data and modeled discharges. J Hydrol 328:481–496

Linacre ET (1977) A simple formula for estimating evaporation rates in various climates, using temperature DATA alone. Agric Meteorol 18:409–424

McFeeters SK (1996) The use of the Normalized Difference Water Index (NDWI) in the delineation of open water features. Int J Remote Sens 17:1425–1432

McSweeney C, New M, Lizcano G, Lu X (2010) The UNDP climate change country profiles improving the accessibility of observed and projected climate information for studies of climate change in developing countries. Bull Am Meteorol Soc 91:157–166

Medina C, Gomez-Enri J, Alonso JJ, Villares P (2010) Water volume variations in Lake Izabal (Guatemala) from in situ measurements and ENVISAT Radar Altimeter (RA-2) and Advanced Synthetic Aperture Radar (ASAR) data products. J Hydrol 382:34–48

Misra A, Balaji R (2015) Decadal changes in the land use/land cover and shoreline along the coastal districts of southern Gujarat, India. Environ Monit Assess. https://doi.org/10.1007/s10661-015-4684-2

Misra A, Murali RM, Vethamony P (2013) Assessment of the land use/land cover (LU/LC) and mangrove changes along the Mandovi–Zuari estuarine complex of Goa, India. Arab J Geosci 8(1):267–279

Muala E, Mohamed YA, Duan Z, Zaag P (2014) Estimation of reservoir discharges from Lake Nasser and Roseires Reservoir in the Nile Basin using satellite altimetry and imagery data. Remote Sens 6(8):7522–7545

Rouse JW, Haas RH, Schell JA, Deering DW (1974) Monitoring vegetation systems in the great plains with ERTS. In: Freden SC, Mercanti EP, Becker MA (eds) Third Earth Resources Technology Satellite-1 Symposium-Volume I: Technical Presentations. NASA, Washington, D.C., pp 309–317

Sundarakumar K, Harika M, Aspiya S, Yamini S (2012) Land use and land cover change detection and urban sprawl analysis of Vijayawada city using multitemporal landsat data. Int J Eng Sci Technol 4:170–178

Swenson S, Wahr J (2009) Monitoring the water balance of Lake Victoria, East Africa, from space. J Hydrol 370:163–176

Zhang R, Zhu D (2011) Study of land cover classification based on knowledge rules using high-resolution remote sensing images. Int J Remote Sens 38(4):3647–3652

Zhang JQ, Xu KQ, Yang YH, Qi LH, Hayashi S, Watanabe M (2006) Measuring water storage fluctuations in Lake Dongting, China, by Topex/Poseidon satellite altimetry. Environ Monit Assess 115:23–37